Jurnal Fizik Malaysia Volume 42 Issue 1 (2021) pgs 10035-10046 D. Ghosh

Positronium Impact Ionization of Sodium Atom with Screened Coulomb Potentials

Dipali Ghosh

Michael Madhusudan Memorial College, Durgapur, West Bengal, India

(Received: 30.5.2021 ; Published: 26.8.2021)

Abstract. The screening effects of Debye-Huckel Potential (DHP) on the positronium (Ps) impact ionization of sodium (Na) atom has been investigated within the framework of the First Born Approximation. The sodium atom is treated as consisting of a positive core (Na^+) and a valence electron (e^-). The interaction of Na^+ and e^- is then approximated by a model potential. The bound state wave functions of Na and Ps are determined variationally by employing simple wave functions. A detailed study has been made on the effects of screening of the DHP on the triple differential cross sections (TDCS) and double differential cross sections (DDCS) for the incident Ps energy ranging from 15 eV to 1000 eV. It is found that TDCS and DDCS suffer considerable changes with changing screening strength.

Keywords: Positronium, Debye- Huckel Potential, model potential, plasma screening

I. INTRODUCTION

Positronium atom (Ps) is the oldest known atom formed by the electron and its anti-particle positron [1]. It is the simplest purely leptonic electromagnetically bound system [2]. Since its discovery by Deutsch [3], the short-lived atom has been the subject of extensive theoretical and experimental studies [2]. It has been used to explore a variety of fundamental phenomena associated with atomic physics, condensed matter physics, astrophysics, industrially important materials, living biological systems [4] etc. As Ps is composed of a particle-anti-particle pair, it is necessary to understand how Ps interacts with other systems. Being a neutral atom, it can penetrate deeper into the system than a charged particle, such as positron. Scattering involving Ps atoms is of importance in the investigations of solar processes [5]. Ps scattering is also important in other branches of physics, such as atomic physics, material science, biophysics [4] etc. So far, the scattering of Ps from a number of atoms and molecules have been investigated. Mention may be made of atoms like H, He, Ne, Ar, Kr, Xe and molecules like H_2, N_2, O_2, CO_2, H_2O, SF_6 [6-13]. Scattering and ionization of Ps from alkali atoms has also been investigated [14- 15]. In this connection, it is important to mention that Laricchia et al [16] have shown that the total cross section in Ps scattering from He, Ne, Ar, Kr, Xe, H_2, N_2, O_2, H_2O, and SF_6 is similar to that of the electron scattering from the corresponding elements within the velocity range 0.5 a.u. to 2.0 a.u.

In this paper we make an attempt to study the ionization of sodium atom (Na) by Ps impact under a screened Coulomb interaction. Specifically, we consider the Debye-Huckel potential. We assume that the interactions among the charged particles in Ps + Na system are governed by the Debye-Huckel potential (DHP) or static screened Coulomb potential (SSCP) of the form (in a.u):

$$V(r)=\frac{e^{-\mu r}}{r} \tag{1}$$

where μ is the screening parameter. Such a study will be useful in the investigations of various astrophysical phenomena [4,5], as most of the astrophysical environments exist in the state of plasma. In plasma environments, the field of potential of test charge is screened due to collective effect of correlated many-particle interactions [17-19]. The properties of an atomic system, embedded in a plasma, suffer considerable changes due to the screening effect of plasma. In many cases the screening of potential in plasmas can be modeled by an effective potential. For example, in a weakly non-ideal plasma, wherein the average thermal energy of the plasma particles dominates over the average inter-particle interactions, the screened potential can be adequately represented by the DHP in the form of equation (1). The screening parameter μ is related with the plasma parameters, such as temperature and density. In many astrophysical media, such as in inertial confinements, compact objects, plasmas are found in weakly non-ideal state with μ varying from 0 a_0^{-1} to 0.8 a_0^{-1} approximately [20]. The condition of weak non-ideality is also satisfied for a wide class of laboratory plasma. So, the DHP can be used to represent the screened interactions in such media.

In vacuum, the ionization of Na by positron and positronium has been investigated by many authors [21-30], which revealed many interesting features. In this work, we use the First Born Approximation (FBA) to study the ionization of Na by Ps under DHP. Our endeavour will be to make a detailed study on the effects of screening of the interaction potentials on the ionization cross section. Carrying out a fully quantum mechanical calculation for Ps impact ionization of Na in a screening environment presents multiple difficulties. The difficulties are mostly associated with the lack of knowledge of exact wave functions of Na and Ps in a screened environment. Here, we treat the sodium atom as consisting of a frozen core and a valence or active electron. The wave functions and eigen energies are then determined within the framework of the method of model potential. Moreover, we resort to a simple variationally determined wave function of Ps. It is to be mentioned that the present target ionization is different from the pure single ionization of Na [27], as in screening environments the effective model potential is changed due to short range of the DHP and also the Coulomb term corresponding to the interaction between nucleus and the scattered electron in vacuum is omitted to consider the screening effect.

II. Theory

We consider the following ionization process:

$$Ps(1s)+Na(3s) \rightarrow Ps(1s) + Na^{+} + e \tag{2}$$

in which interaction of the constituents charged particles are governed by the DHP potential in the form of Eq. (1). Let $\vec{r}_1$, $\vec{r}_2$ and $\vec{r}_3$ denote the coordinates of the positron, the electron in Ps and the active electron in Na respectively, and $\vec{r}_{13} = \vec{r}_1 - \vec{r}_3$, $\vec{r}_{23} = \vec{r}_2 - \vec{r}_3$ and $\vec{R} = \frac{1}{2}(\vec{r}_1 + \vec{r}_2)$. As stated above, we treat the sodium atom as consisting of a frozen core (Na^+) and a valence or active electron. The wave function and eigen energies of the Na are then determined within the framework of the method of model potential. In the present work, we consider the following model potential to represent the interaction between the core and the electron [31, 32]:

$$V_{mod}^{(e^-)}(\vec{r}_i) = -\frac{e^{-\mu r_i}}{r_i}\,[1 + 10(e^{-2\alpha r_i} + \beta r_i e^{-2\gamma r_i})],\ i = 2,3 \quad (3a)$$

The above model potential which was used by Masanta *et al* [32] in the study of resonances in positronic sodium atom is so chosen that it simulates the multi-electron core interaction with the single valence electron in an analytic modification of the Coulomb potential. The values of the parameters $\alpha\ (= 1.8321)$, $\beta\ (= 1.0591)$ and $\gamma\ (= 1.3162)$ are determined by solving the corresponding one-electron Schrodinger equation within the framework of the Rayleigh-Ritz variational principle so that the eigen energies agree with the experimental results of the bound state energies of the Na. For positron-core interaction, we have used the same model potential with opposite sign, that is,

$$\mathrm{V}_{\mathrm{mod}}^{(\mathrm{e}^+)}(\vec{r}_1) = \frac{\mathrm{e}^{-\mu \mathrm{r}_1}}{\mathrm{r}_1}\,[1 + 10(\mathrm{e}^{-2\alpha \mathrm{r}_1} + \beta \mathrm{r}_1 \mathrm{e}^{-2\gamma \mathrm{r}_1})] \quad (3b)$$

This makes the positron-core interaction a bit more repulsive than the actual interaction, as the model potential (Eq.3a) includes the effects of electron exchange. The complexity in working with many-electron atoms that prevailed in different theoretical investigations [33-38] has been circumvented by considering the model potential [39, 40], where the effect of the core electrons have not been considered explicitly.

With these description the non-relativistic Hamiltonian (in a.u.) of the Ps + Na system interacting with the DHP is given by,

$$H = -\frac{\nabla_R^2}{2\mu_i} - \frac{\nabla_{12}^2}{2\mu_{Ps}} - \frac{\nabla_3^2}{2} - \frac{1}{r_{12}} + \mathrm{V}_{\mathrm{mod}}^{(\mathrm{e}^+)}(\vec{r}_1) - V_{mod}^{(e^-)}(\vec{r}_2) - V_{mod}^{(e^-)}(\vec{r}_3) - \frac{e^{-\mu r_{13}}}{r_{13}} + \frac{e^{-\mu r_{23}}}{r_{23}} \quad (4)$$

where μ_i and μ_{Ps} are the three body reduced mass in the initial channel and the reduced mass of the positronium atom respectively.

In the initial and the final channel, H can be split as:

$$H = H_i + V_i = H_f + V_f \quad (5)$$

such that $$H_i\Phi_i = E_i\Phi_i \ \text{ and } \ H_f\Phi_f = E_f\Phi_f \quad (6a)$$

Where Φ_i and Φ_f are the unperturbed states corresponding to the Hamiltonians H_i and H_f respectively, with residual interactions V_i and V_f having energies

$$E_i = k_i^2 + \varepsilon_{Ps} + \varepsilon_{Na} \quad \text{and} \quad E_f = k_f^2 + k_3^2/2 + \varepsilon_{Ps} \quad (6b)$$

Here $\vec{k}_i$, $\vec{k}_f$ are the momentum of Ps in the initial channel and final channel respectively, and $\vec{k}_3$ is momentum of the ejected electron. In this equation ε_{Na}, ε_{Ps} represent the binding energies of Na (3s) and Ps (1s) atom respectively. The scattering amplitude, in the FBA, for the ionization process (Eq. 2) is given by,

$$T_{if}(\vec{k}_i, \vec{k}_f, \vec{k}_3) = -\frac{\mu_f}{2\pi}\left\langle \Phi_f(\vec{r}_1, \vec{r}_2, \vec{r}_3)\,\middle|V_i\middle|\,\Phi_i(\vec{r}_1, \vec{r}_2, \vec{r}_3)\right\rangle \text{ (prior form)} \quad (7a)$$

$$T_{if}(\vec{k}_i, \vec{k}_f, \vec{k}_3) = -\frac{\mu_f}{2\pi}\left\langle \Phi_f(\vec{r}_1, \vec{r}_2, \vec{r}_3)\,\middle|V_f\middle|\,\Phi_i(\vec{r}_1, \vec{r}_2, \vec{r}_3)\right\rangle \text{ (post form)} \quad (7b)$$

In the present work we have adopted the prior version of the scattering amplitude as given by equation (7a) which is supposed to be more suitable for an ionization process [41- 44]. Equation

(7) concerning a four body problem could not be solved exactly and as such one has to resort to some simplifying assumptions.

For the present case, Φ_i and Φ_f are respectively given by

$$\Phi_i(\vec{r}_1, \vec{r}_2, \vec{r}_3) = \varphi^{Ps}(\vec{r}_{12})\, e^{i\vec{k}_i.\vec{R}}\ \varphi_{3s}^{Na}(\vec{r}_3) \tag{8a}$$

$$\Phi_f(\vec{r}_1, \vec{r}_2, \vec{r}_3) = \varphi^{Ps}(\vec{r}_{12}) e^{i\vec{k}_f.\vec{R}} N_3 (2\pi)^{-3/2} e^{i\vec{k}_3.\vec{r}_3}\ \ {}_1F_1\left(-i\alpha_3, 1, -i\left(k_3 r_3 + \vec{k}_3.\vec{r}_3\right)\right) \tag{8b}$$

where φ^{Ps} and φ_{3s}^{Na} respectively denote the ground state wave functions of Ps and Na, and α_3 is the Coulomb phase lag or the Sommerfeld parameter. In the present work we determine φ^{Ps} and φ_{3s}^{Na} variationally by employing the following trial radial wave functions:

$$\varphi^{Ps}(r_{12}) = \frac{\lambda_{Ps}^{3/2}}{\sqrt{\pi}} \exp(-\lambda_{Ps} r_{12}) \tag{9a}$$

$$\varphi_{3s}^{Na}(\vec{r}_3) = \left(\frac{1}{4\pi}\right)^{1/2} \left[2(\lambda_{Na})^{3/2} e^{-\lambda_{Na} r_3} - 4\,(\lambda_{Na})^{5/2} r_3 e^{-\lambda_{Na} r_3} + \frac{4}{3}(\lambda_{Na})^{7/2} e^{-\lambda_{Na} r_3}\ r_3^2\right] \tag{9b}$$

where λ_{Ps} and λ_{Na} are variational parameters determined by optimizing the corresponding Rayleigh-quotient. It is to be noted that in the final channel, the ejected electron moves in the field of Na^+ which, for the unscreened case (μ=0), is a long-range Coulombian field. But, when the interaction potential gets screened ($\mu \neq 0$), it eventually becomes short-range. The long-range Coulombian field is taken care of by the confluent hypergeometric function (${}_1F_1$) for μ =0. We set α_3= 0 for $\mu \neq 0$ so that it leads to the short-range potential.

In order to avoid the complexity in the analytical calculations, we have neglected the higher order interactions between the e^+ / e of the Ps and the target electron and have mainly concentrated on the ionization of the target; this interaction being considered through the perturbation interaction in the initial channel.

After performing some algebra and calculus [45- 49], the ionization amplitudes T_{if} in Eq. (7a) is finally reduced to a three dimensional numerical integral. Having obtained T_{if}, the triple differential cross sections (TDCS) [48] and the double differential cross sections (DDCS) can be calculated by using the standard relations, namely the TDCS is given by

$$\frac{d^3\sigma}{dE_3 d\Omega_f d\Omega_3} = \frac{k_f k_3}{k_i} \left|T_{if}\right|^2 \tag{10}$$

and the DDCS, $\frac{d^2\sigma}{dE_3 d\Omega_f}$ are obtained by integrating over the solid angle $d\Omega_3$.

In this context it may be mentioned that due to the principle of detailed balance, the transition amplitudes obtained from the post and prior forms should, in principle, be the same if the exact scattering wave functions in the initial or final channel are used, which for a four body problem is a formidable task. In the case of approximate wave functions, the aforesaid post and prior forms might not lead to identical results giving rise to some post–prior discrepancy.

III. Results and Discussions

The TDCS and the DDCS are computed for single ionization of Na by Ps under DHP. For the single ionization, the threshold energy is determined by, $E_{th} = \varepsilon_{Na}$. Since the present study is made in coplanar geometry, that is $\vec{k}_i$, $\vec{k}_f$ and $\vec{k}_3$ all in the same plane, the azimuthal angles $\emptyset_i$, $\emptyset_f$ and $\emptyset_3$ can assume values 0^0 and 180^0. In few cases, TDCS has been calculated by adopting the following convention for the scattered angles, $(\theta_f, \emptyset_f)$: $(\theta_f, 0^0)$ is taken as $-|\theta_f|$ (recoil region), while $(\theta_f, 180°)$ is taken as $|\theta_f|$ (binary region).

Figure 1 exhibits TDCS in atomic unit (a.u.) of the ejected electron with scattering angle θ_3 for the single ionization. To study the effect of screening of DHP on the TDCS of single ionization of sodium, four different values of screening parameter μ (a_0^{-1}) are chosen under four different kinematics. Keeping the scattering angle of the Ps fixed at θ_f = 35^0, the incident energy and the ejected energy are varied. From Figure 1, it is clear that TDCSs are more responsive to the screening for lower incident energies.

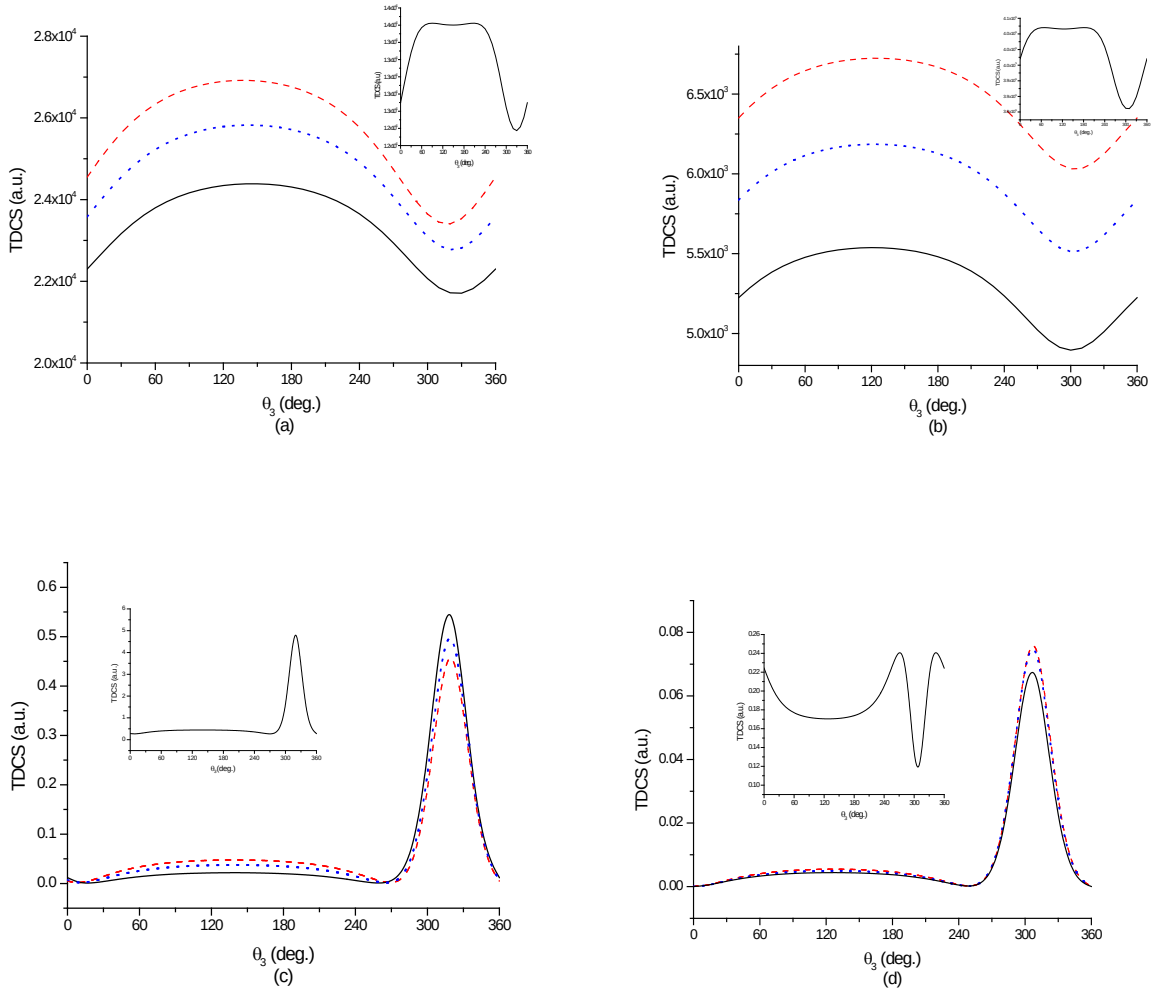

FIGURE 1. TDCS as a function of ejected electron angle (θ_3) for different values of the screening parameter μ (in a_0^{-1}) and for four different kinematics. (a) E_i = 15 eV, E_3 = 5 eV and $\theta_f = 35^0$, (b), E_i = 30 eV, E_3 = 5 eV and $\theta_f = 35^0$, (c), E_i = 100

eV, E_3 = 50 eV and $\theta_f = 35^0$ and (d) , E_i = 150 eV, E_3 = 50 eV and $\theta_f = 35^0$. Inset curves correspond to μ = 0, red dashed curves correspond to μ= 0.02, blue dotted curves correspond to μ= 0.05 and black solid curves correspond to μ= 0.1.

At low incident energies substantial change in the TDCS is observed due to effect of screening. In contrast, at high incident energies, change in the TDCS due to the increasing screening strength is small. More interestingly, the pattern of the TDCS in vacuum at 150 eV is changed due to the effect of screening. Furthermore, the change of peak in the TDCS due to the effect of screening depends on the incident energy as well as on the kinematics. At low incident energies, the peak is reduced with increasing screening strength. However, at high incident energies, combined effects of screening and kinematics lead to the change in the peak in TDCS, as is evident from Figure 1(c) and 1(d). The present unscreened TDCS (inset curve of fig. 1d) shows mostly similar qualitative behaviour with a slight reduced magnitude while comparing with the three Coulomb (3C) result of positron impact ionization of Na [30] for E_i =150 eV .

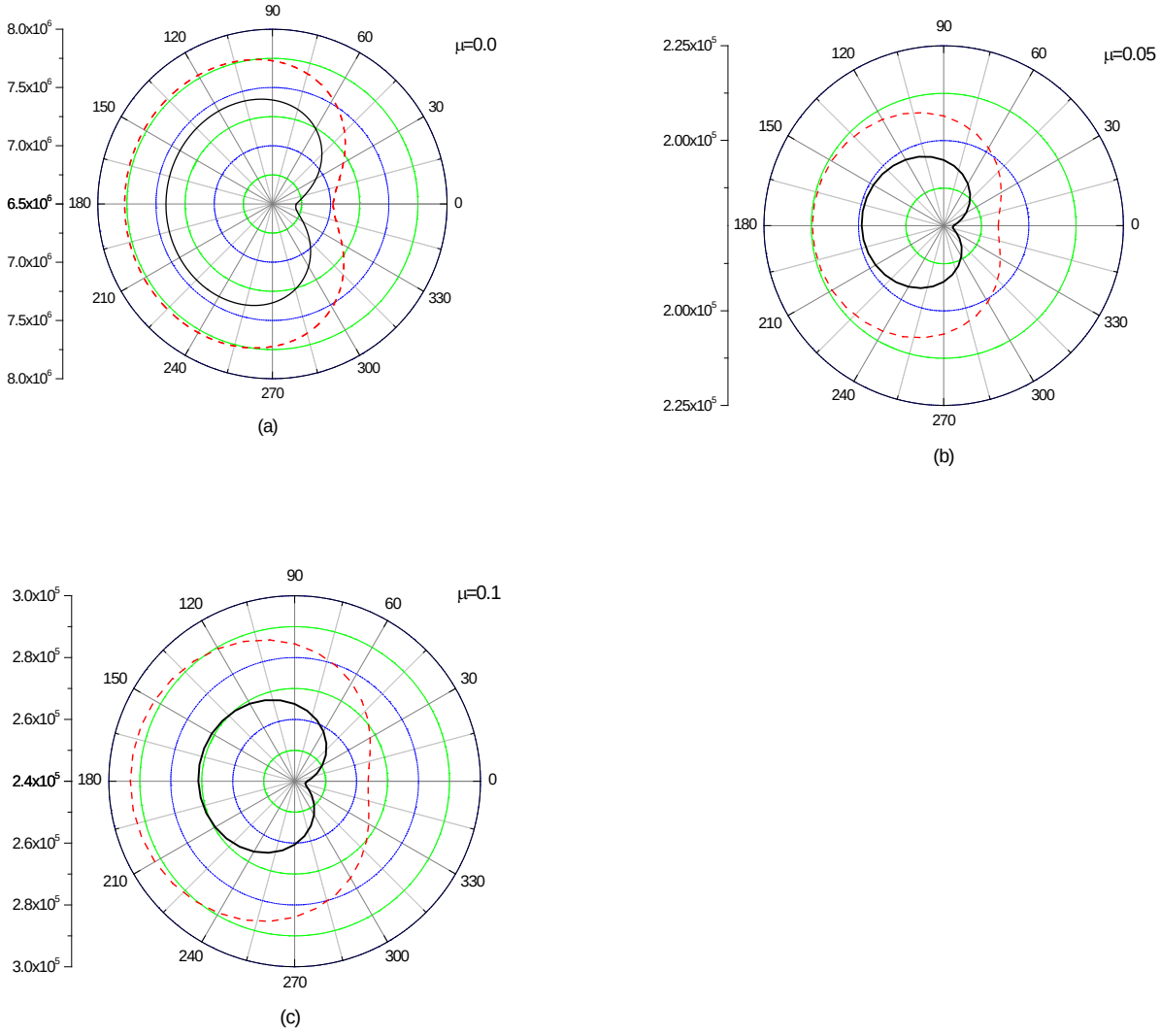

FIGURE 2. TDCS as a function of the ejected electron angle (θ_3) for different scattering angles (θ_f) and screening strengths μ (in a_0^{-1}) for fixed incident energy 15 eV and ejected energy 5 eV. Dashed (red) curves are for $\theta_f = 0.5^0$ and solid (black) curves are for $\theta_f = 5.0^0$. (a) μ= 0.0 , (b) μ= 0.05 and (c) μ= 0.1.

Figure 2 shows the TDCS as a function of the angle made by the ejected electron with incident direction, at 15eV incident energy for two different scattering angles (0.5^0 and 5^0) and for three screening strengths (μ = 0, 0.05 and 0.1 a_0^{-1}). From Figure 2 we notice that magnitude of the TDCS is higher for 0.5^0 than for 5^0. Furthermore, with the increasing screening strength, magnitude of the TDCS first decreases then gradually increases. A small kick is observed near $\theta_3 = 0^0$. This kick is prominent for the unscreened case. It seems that TDCS as a function of θ_3 not only depends on the incident energy and screening strength for given values of the scattering angles, but also depends on the kinematics of the whole process.

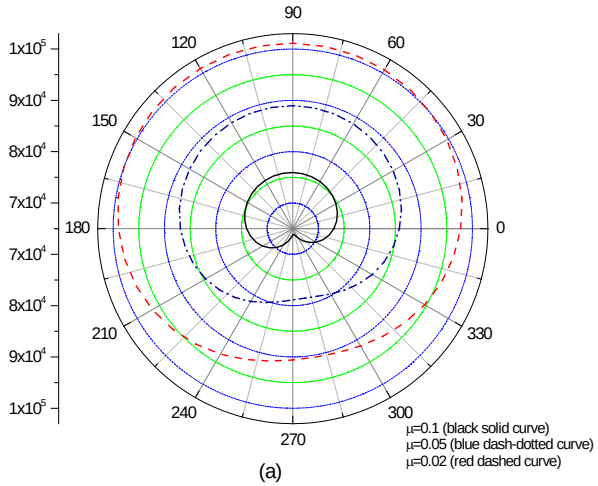

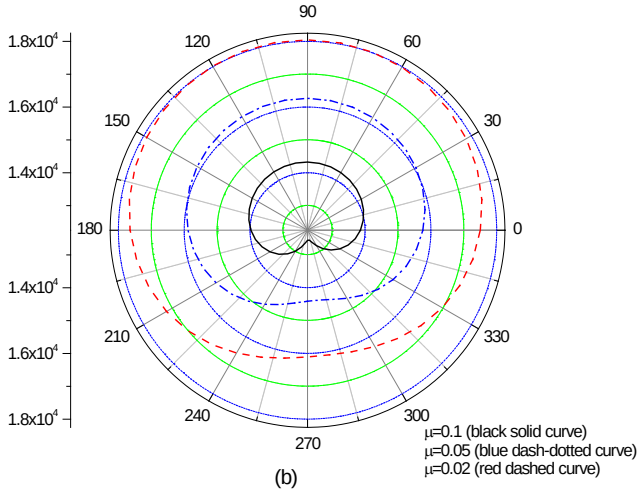

FIGURE 3. TDCS as a function of ejected electron angle (θ_3) for two incident energies, (a) 500 eV and (b) 1000 eV respectively for fixed ejected energy 5 eV and $\theta_f = 5.0^0$. μ= 0.02 is represented by red dashed curve, μ= 0.05 is represented by blue dash - dotted curve and μ= 0.1 is represented by black solid curve.

In Figure 3, the incident energy is raised to 500eV and higher, and the effect of screening on the TDCS (as a function of ejected electron angle for a given scattering angle) is examined. We find TDCS is reduced due to the effect of screening. Moreover, in comparison to Figure 2, the kick is shifted to $\theta_3 = 270^0$, and it is prominent for $\mu = 0.1\ a_0^{-1}$.

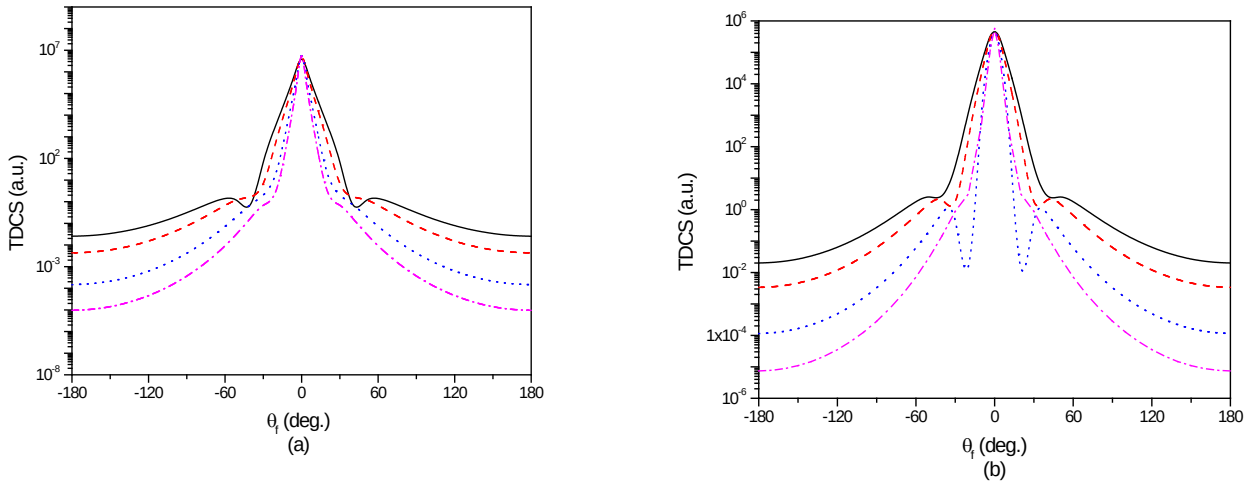

FIGURE 4. TDCS as a function of the scattered positronium angle (θ_f) for four incident energies, 100 eV (black solid curve), 150 eV (red dashed curve) , 300 eV (blue dotted curve) and 500 eV (magenta dash dotted curve). Ejected energy is fixed at 5 eV and $\theta_3 =$ 0.50. (a) μ= 0.05 and (b) μ= 0.1

The change in the TDCS as a function of the scattering angle due to the effect of screening is put up in Figure 4. We notice that the pattern of the TDCS is almost the same for each of the incident energy. However, the TDSC decreases with respect to the increasing incident energy. Furthermore, when screening strength is increased, TDCS is found to be reduced.

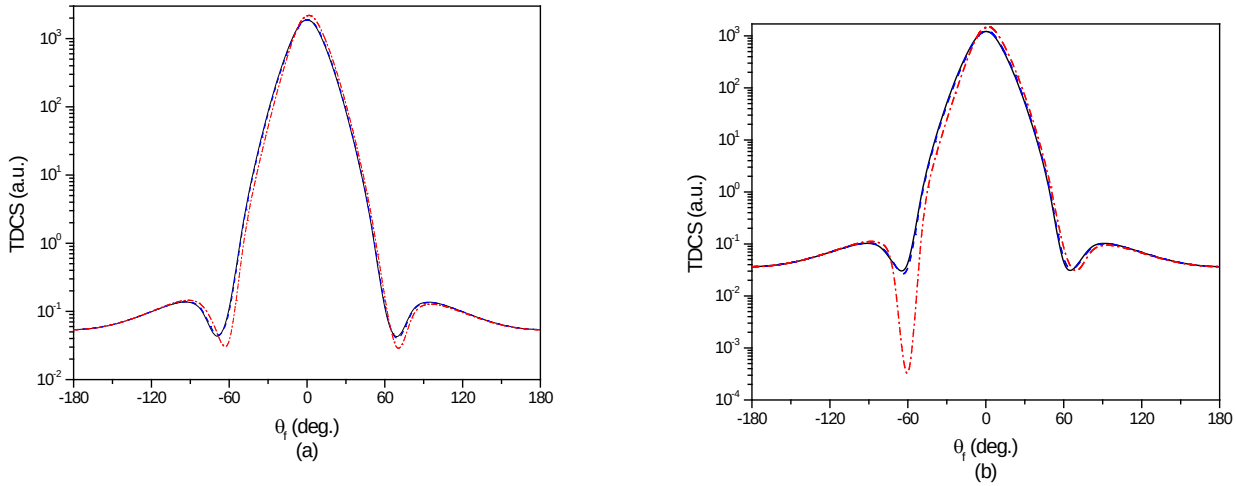

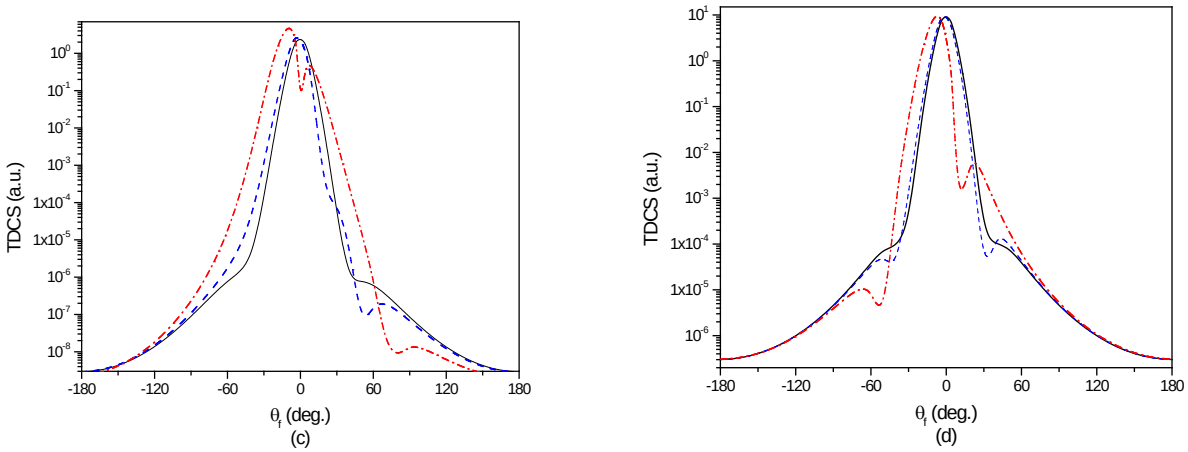

FIGURE 5. TDCS as a function of scattered positronium angle (θ_f) for four different set of kinematics. (a) $E_i = 50\ eV, E_3 = 23\ eV, \mu = 0.05$ (b) $E_i = 50\ eV, E_3 = 23\ eV, \mu = 0.1$ (c) $E_i = 168.4\ eV, E_3 = 54.4\ eV$, $\mu = 0.05$ (d) $E_i = 168.4\ eV, E_3 = 54.4\ eV, \mu = 0.1$, In all figures $\theta_3 = 0.5^0$ (black solid curve), $\theta_3 = 5^0$ (blue dashed curve) , $\theta_3 = 30^0$ (red dash- dotted curve).

To study the effect of screening on the symmetric kinematics, equal energy sharing of ejected electron and scattered Ps is considered, as shown in Figure 5. In particular, two different incident energies, $E_i = 50$ eV (Figure a and b), and 168.4 eV (Figure c and d) and for two different values of the screening parameter, μ =0.05 and 0.1 a_0^{-1} are considered in Figure 5. For these two sets of kinematics ejected electron angle is also varied. As noted from these figures, for lower ejection angle of electron, scattering of Ps in forward direction is preferred irrespective of incident energies and screening parameter. Again, for symmetric kinematics, TDCS is raised due to the increasing screening strength for higher incident energies. However, the opposite effect is seen for lower incident energies. The event of velocity matching is studied (figs. c and d) for the incident energy $E_i = 168.4\ eV$. It should be pointed out that the mass of the Ps is twice the mass of the electron. Thus, we have considered the energy of the ejected Ps twice the energy of the ejected electron to keep pace between ejected electron and Ps in velocity space. For this kinematics, it is observed that the peak on the TDCS (θ_f) are almost similar for smaller ejection angles of the electron (θ_3), whereas the TDCSs for larger values of $\theta_3(30^0)$ show a different behaviour than that of the forward ejection. Furthermore, for all the kinematics, screening effect is also appreciable for higher ejection angles (such as θ_3=30^0) than that of forward ejection (θ_3=0.5^0 & 5^0).

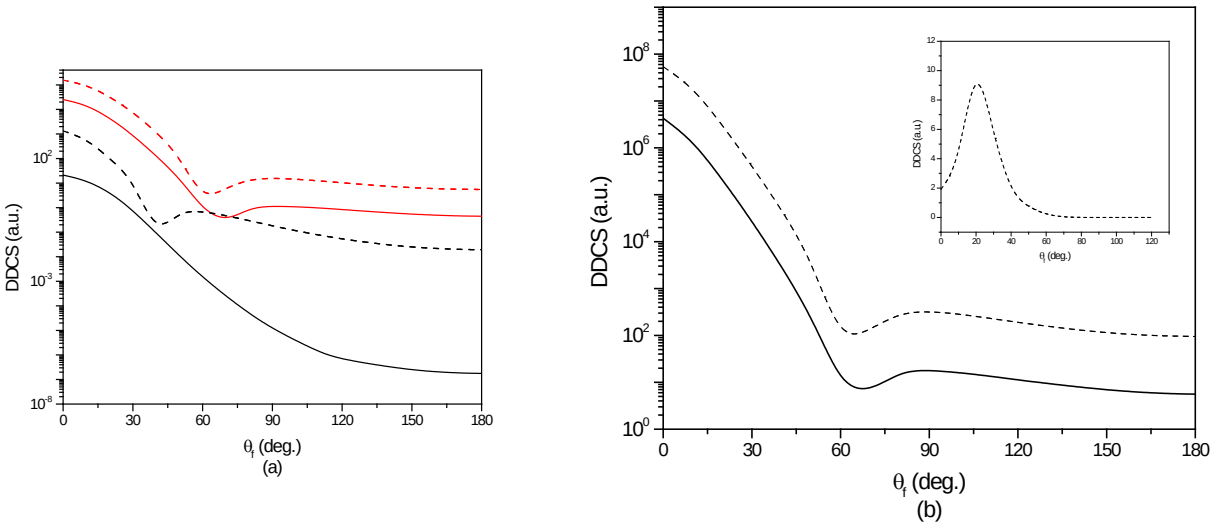

FIGURE 6. DDCS as a function of θ_f for two different kinematics and for two different μ. (a) Red dotted curve: $E_i = 50\ eV, E_3 = 23\ eV, \mu = 0$, Red solid curve: $E_i = 50\ eV, E_3 = 23\ eV, \mu = 0.1$ Black dotted curve: $E_i = 106\ eV\ eV, E_3 = 50\ eV, \mu = 0$. Black solid curve: $E_i = 106\ eV\ eV, E_3 = 50\ eV, \mu = 0.1$; (b) Black dotted curve: $E_i = 45\ eV\ eV, E_3 = 10\ eV, \mu = 0$. Black solid curve: $E_i = 45\ eV\ eV, E_3 = 10\ eV, \mu = 0.1$. Inset figure $E_i = 45\ eV\ eV, E_3 = 10\ eV, \mu = 0$ of [27].

Figures 6a and 6b exhibit the double differential cross sections (DDCS) as a function of scattered Ps angle θ_f. Figure 6a shows the distribution of the scattered Ps at the incident energies, 106 eV and 50 eV, where the energy of the ejected electron is kept fixed at 50 eV and 23 eV respectively while figure 6b, depicts the curves for incident energies 45 eV and ejected electron energy 10 eV. It is clear from the figures that the DDCS is reduced due to the effect of the screening which is prominent for higher incident energy. Kinematics of figure 6b allow us to compare the unscreened results with existing calculation [27]. It is noted from the figure that, DDCS of the present calculation is much greater than that of the previous calculation for this kinematics and maxima shifted towards lower scattering angle than that was in DDCS distribution of [27] (vide inset figure). These differences in the DDCS between the present and the existing work [27], may be the consequence of two factors. Firstly, ground state (3s) wave function of Sodium atom considered in the present case, which was chosen in the form of a simple hydrogenic orbital in the existing work [27] and secondly, the final state wave function considered in present case is a simplified one in absence of any higher order interactions between target nucleus and two components of positronium, which was taken in consideration in the existing work [27] by introducing the two eikonal factors in the final state wave function.

IV. Conclusions

In summary, we make an attempt to study the effects of the screening of the Debye-Huckle potential on the ionization of the sodium atom by Ps impact. We find that screening of the Debye-Huckel potential causes substantial changes in TCDCs and DDCSs. The changes introduced by the screening not only depend on the incident energy, but the changes depend on the whole kinematic of the scattering system. We hope that our present findings will provide important information to the research in plasma physics, astrophysics and atomic physics.

ACKNOWLEDGMENTS

I would like to convey my sincere gratitude to Prof. Arijit Ghoshal, Department of Mathematics, University of Burdwan, for his immense help and wise guidance in this project.

REFERENCES

1. Stephan Berko and Hugh N. Pendleton, *Ann. Rev. Nucl. Part. Sci*. **30**, 543-81(1980).
2. David B. Cassidy, *J Euro Phys D* **72**,53 (2018).
3. M. Deutsch, *Phys. Rev*. **82**, 455 (1951).
4. G. Laricchia and H.R.J. Walters, Positronium collision physics, *Rivista del Nuovo Cimento* **35** no. 6, 305 (2012).
5. Carol Jo Crannel, Glenn Joyce, Reuven Ramaty, and Carl Werntz *ApJ*, **210** 582–592 (1976)
6. G. Laricchia, M. Charlton, S. A. Davies, C. D. Beling and T. C. Griffith, *J. Physics B,* **20** no.3, L99 (1987).
7. N. Zafar, G. Laricchia, M. Charlton, and A. Garner, *Physical Rev. Letters* **76** no. 10, 1595 (1996).
8. A. J. Garner, G. Laricchia, and A. Ozen, *J.Phys. B*, **29** no. 23, 5961 (1996).
9. G. Laricchia, S. Armitage, A. Kov¨er, and D.J. Murtagh, "Ionizing Collisions by Positrons and Positronium Impact on the Inert Atoms ", *Advances In Atomic, Molecular and Optical Physics*, Elsevier BV. 56 (2008) p. 1.204.
10. A. J. Garner, A. Ozen, and G. Laricchia, *J.Phys.B* **33** no. 6, 1149 (2000).
11. S. Armitage, D. E. Leslie, A. J. Garner, and G. Laricchia, *Physical Review Letters* **89** no. 17, 173402 (2002).
12. J. Mitroy and I. A. Ivanov, *Phys. Rev. A* **65**, 012509 (2001).
13. A. Ivanov, J. Mitroy, and K. Varga, *Phys. Rev. A* **65**, 022704 (2002).
14. H. R. J. Walters, A.C.H. Yu , S.Sahoo ,Sharon Gilmore, *Nuclear Instruments and Methods in Physics Research Section B,* 221, 149-159 (2004).
15. Sukanya Sur, Sadhan K. Adhikari, and A. S. Ghosh, *Phys. Rev. A* 53, 3340 (1996)
16. S. J. Brawley, S. Armitage, J. Beale, D. E. Leslie, A. I. Williams, G. Laricchia, *Science* **330**, 789 (2010).
17. D. Salzmann, Atomic Physics in Hot Plasmas, Oxford, Oxford University Press, 1998.
18. M. S. Murillo, and J. C. Weisheit, *Phys. Rep*. **302**, 1 (1998).
19. Hansen, and I. McDonald, Theory of simple liquids, London, Academic Press 1986.
20. N. Masanta and A. Ghoshal, *Chin J. Phys*. **71**, 273 (2021).
21. Igor Bray, *Physics Review Letter* **73**, 1088 (1994).
22. Wayne K. Trail et al *Physics. Rev. A* **49,** 3620 (1994).
23. G. S. J. Armstrong, J. Colgan, M. S. Pindzola, *Physics. Rev. A* **88,** 042713 (2013).
24. Sushma, Praveen Bhatt and S. P. Gupta, *IRJMST***, 8** 2348 (2017).
25. K. Mukherjee, N. Ranjit Singh, Keka Basu Choudhury, P. S. Mazumdar, *Physics. Rev. A*, **46** 234 (1992).
26. Zhon Ya jun, Pan Shou-pu, Chinese *Physics Letters*, **14** (9) 348 (2008).
27. D. Ghosh, *Journal of Atomic, Molecular, Condensate & Nano Physics* **5**, No. 1. 55–66, (2018)
28. I E McCarthy, K Ratnavelu and Y Zhou, *J. Phys. B.* **26**, 2733 (1993).
29. Nithyanandan Natchimuthu and Kuru Ratnavelu, *Phys. Rev. A* **63**, 052707 (2001).

30. R. Cheikh, J. Hanssena, and B. Joulakian *Eur. Phys. J. D* **2**, 203- 208 (1998).
31. Arijit Ghoshal and Yew Kam Ho, *Physical Review A*, **95**, 052502 (2017).
32. N. Masanta, A. Ghoshal, & Y. K. Ho, *Indian J Phys* **94**, 1495–1503 (2020).
33. S. Guha and P. Mandal, *J. Phys. B: At. Mol. Opt. Phys*. **13**, 1919 (1980).
34. C. Sinha, S. Guha and N. C. Sil, *J. Phys. B: At. Mol. Opt. Phys*. **15** ,1759 (1982).
35. P. Cavaliere, G. Ferrente and B.M. Montes, *Chem. Phys. Lett*. **36**, 583(1975).
36. G. Bordonaro, G. Ferrante, M. Zarcone and P. *Cavaliere, Nuovo. Cim. B* **35**, 349 (1976).
37. G. Ferrante, L.O. Cascio and M. Zarcone, *Nuovo. Cim. B* **44**, 99 (1978).
38. B. M. Montes, P. Cavaliere and G. Ferrante, *Chem. Phys. Lett*. **32**, 469(1975).
39. P. Cavaliere and G. Ferrante, *Nuovo. Cim. B* **14**, 127(1973).
40. J. Hanssen, R. McCarroll and P. Valiron, *J. Phys. B* **12** ,899 (1979).
41. Brauner, J. Briggs and H. Klar, *J. Phys. B* **22**, 2265 (1989).
42. R. Biswas and C. Sinha, *Phys. Rev. A* **50**, 354 (1994).
43. S. Roy, D. Ghosh and C. Sinha, *J. Phys. B* **38**, 2145 (2005).
44. S. Roy and C. Sinha, *Phys. Rev. A* **80**, 022713 (2009).
45. C. Sinha and N. C. Sil, *J. Phys. B* **11**, L333 (1978).
46. B. Nath and C. Sinha, *J. Phys. B* **33**, 5525 (2000).
47. D. Ghosh and C. Sinha, *Phys. Rev. A* **69**, 052717(2004).
48. D. Ghosh and C. Sinha, *Indian Journal of Physics* **90**, 973 (2016).
49. Avaldi, P. Camilloni and G Stefani, *Phys. Rev. A* **41**,134 (1990).